Modern Physics Letters A

STUDY OF THE DIJET INVARIANT MASS IN W+JETS EVENTS BY THE DØ COLLABORATION

JADRANKA SEKARIC *

Department of Physics and Astronomy, University of Kansas,
1082 Malott, 1251 Wescoe Hall Drive, Lawrence, Kansas 66045, USA
sekaric@fnal.gov

Received (23 November 2011)
Revised (Day Month Year)

The recent claim by the CDF Collaboration of a possible anomalous dijet resonance in their data required experimental verification from other hadron collider experiments. We present a study of the dijet invariant mass spectrum in events with two jets produced in association with a $W \to \ell\nu$ boson at the DØ experiment. We investigate the dijet mass range between 110 GeV/c^2 and 170 GeV/c^2 and find no evidence for any resonant dijet production.

Keywords: Dijet mass; resonant production; confidence level limits.

PACS Nos.: 12.15.Ji, 12.38.Qk, 13.85.Rm, 14.80.-j

1. Introduction

The production of two highly energetic jets of particles is very well described within the standard model (SM) of particle physics by the quantum field theory of strong interactions. For jet production associated with the production of a W boson, there are several SM processes that share the same signature, such as diboson production, W+jets production, and associated production of W boson and the light Higgs boson. However, in the presence of new physics, there could be additional contributions from the production of a new particle that decays into a dijet final state as suggested in Ref. 1 - 3.

Recently, the CDF Collaboration at the Fermilab Tevatron $p\bar{p}$ collider with $\sqrt{s} = 1.96$ TeV reported a significant excess of events in the dijet invariant mass distribution at $M_{jj} = (144 \pm 5)$ GeV/c^2 as presented in Ref. 4. The excess, with a statistical significance of 3.2 standard deviations (s.d.) above the background expectation, was isolated in data corresponding to an integrated luminosity of 4.3 fb^{-1} after tightening the event selection criteria from a previous $WW + WZ$ production study (see Ref. 5). The analyzed $WW + WZ$ final states consist of the W boson

*Fermilab, M.S. 352, P.O. Box 500, Batavia, Illinois 60510-5011, USA

Operated by Fermi Research Alliance, LLC under Contract No. De-AC02-07CH11359 with the United States Department of Energy.

decaying leptonically, $W \to \ell\nu$, where $\ell = e$ (electron) or μ (muon), and the associated W or Z boson decaying into jets, $W/Z \to jj$. An updated CDF analysis with additional integrated luminosity of 3 fb^{-1} confirmed the presence of the excess in the dijet mass spectrum with the significance of 4.1 s.d., as described in Ref. 6. Assuming that this excess represents a resonant production of a hypothetical particle X, with a branching ratio for a dijet decay mode $\mathrm{BR}(X \to jj) = 1$, this excess is modeled as a dijet resonance with a width $\sigma_{jj} = 14.3$ GeV/c^2 dominated by the detector resolution. The acceptance and selection efficiency for the associated production of this hypothetical WX signal is modeled with $WH \to \ell\nu b\bar{b}$ Monte Carlo (MC) events, where the Higgs boson, H, decaying into $b\bar{b}$ pair is generated with a mass of 150 GeV/c^2. Based on these assumptions, the CDF Collaboration reports an estimated production cross section of $\sigma(p\bar{p} \to WX) \approx 4$ pb.

To verify the CDF findings we analyze a dataset corresponding to an integrated luminosity of 4.3 fb^{-1} collected with the DØ detector and emulate the CDF event selection as closely as possible, to probe the DØ data for an existence of an anomalous dijet mass resonance in a wide M_{jj} range.

2. Event Selection

The $\ell\nu jj$ final state is characterized by a highly energetic charged lepton (electron or muon), missing transverse energy due to the presence of a neutrino, and two highly energetic hadronic jets. The selection criteria we apply to select these final states are dictated by the choices made by the CDF Collaboration. Thus, we require that each event contains a single reconstructed electron or muon with transverse momentum $p_T > 20$ GeV/c and pseudorapidity $|\eta| < 1.0$, where $\eta = -\ln[\tan(\theta/2)]$ with θ being the polar angle measured with respect to the proton beam direction. To improve the purity of the selected leptons we require the leptons to be spatially matched to a track reconstructed in the central tracking detector that originates from the $p\bar{p}$ interaction vertex, and that it is isolated from other energy depositions in the calorimeter and other tracks in the central tracking detector. For electrons we require $(E_{tot}(0.4) - E_{em}(0.2))/(E_{em}(0.2)) \leq 0.07$ where $E_{tot}(0.4)$ $(E_{em}(0.2))$ is the total (electromagnetic) energy in a cone of radius $\Delta R = \sqrt{(\Delta\eta)^2 + (\Delta\phi)^2} \leq 0.4$ (0.2), with ϕ being the azimuthal angle measured with respect to the proton beam direction. We also require the sum of the p_T of tracks in hollow cone with $0.05 < R < 0.4$ around the electron to be less than 2.5 GeV. For muons we require that both the sum of the p_T of tracks within $\Delta R \leq 0.5$ and the sum of calorimeter clusters around the muon within $0.1 \leq R \leq 0.4$ each are less than 2.5 GeV.

The missing transverse energy per event is required to be $\not\!\!E_T > 25$ GeV. To reduce the background from processes that do not contain $W \to \ell\nu$ decays, we require the transverse mass $M_T^{\mu\nu} = \sqrt{2p_T^l \not\!\!E_T(1 - cos)\Delta\phi}$, reconstructed from the charged lepton and $\not\!\!E_T$, to be $M_T^{\ell\nu} > 30$ GeV/c^2. In addition, in the muon channel we restrict $M_T^{\mu\nu} < 200$ GeV/c^2 to suppress the contribution from muons with poorly measured momenta.

Regarding jets, we select events with exactly two jets reconstructed using a jet cone algorithm with a cone of radius $\Delta\mathcal{R} = 0.5$ (see Ref. 7). Jets in CDF are reconstructed within a cone of radius $\Delta\mathcal{R} = 0.4$, which is a difference between the CDF and DØ jet reconstruction algorithms driven by the specifics of each detector. Further, we require that exactly two reconstructed selected jets satisfy $p_T > 30$ GeV/c, while events with additional jets with $p_T < 30$ GeV/c are also accepted. To increase the probability of selecting jets that originate from the hard scattering process in data collected at high luminosities, we require that the reconstructed jets contain two or more tracks originating from the $p\bar{p}$ interaction vertex. The two jets reconstructed within pseudorapidity $|\eta_j| < 2.5$ and with total transverse momentum of the dijet system of $p_T(jj) > 40$ GeV/c, are mutually separated by $|\Delta\eta(jj)| < 2.5$. In addition, the most energetic jet must be separated from the direction of the $\not\!\!E_T$ by an azimuthal angle of $\Delta\phi(j, \not\!\!E_T) > 0.4$.

3. Modeling of Standard Model Processes

We model most of the SM processes decaying in the $\ell\nu jj$ final states using MC simulations. To simulate inclusive WW, WZ and ZZ (diboson) production we use PYTHIA (see Ref. 8) with CTEQ6L1 parton distribution functions (PDFs) described in Ref. 9 and 10. These samples are normalized to the next-to-leading order (NLO) cross sections calculated with the MCFM (see Ref. 11) event generator. To generate $W(\to \ell\nu)$+jets and $Z(\to \ell\ell)$+jets MC samples, including the light parton (u,d, s or gluon) and heavy-flavor ($c\bar{c}$ or $b\bar{b}$) contributions, we use the ALPGEN (see Ref. 12) generator with CTEQ6L1 PDFs, interfaced to PYTHIA for parton showering and hadronization. The $t\bar{t}$ and single top-quark events are generated with ALPGEN using CTEQ6L1 PDFs, and COMPHEP (see Ref. 13) with CTEQ6M PDFs, respectively, both interfaced to PYTHIA. The Z+jets events are normalized to the next-to-NLO cross section from FEWZ (see Ref. 14) while the additional NLO heavy-flavor corrections, calculated with MCFM (see Ref. 15), are applied to Z/W+heavy-flavor jets MC samples. The $t\bar{t}$ and single top-quark events are normalized to the approximate NNLO and NLO cross sections, respectively (see Ref. 16 and 17). The normalization of the dominant W+jets contribution is determined from data. More precisely, the W+jets sample is normalized to the LO cross section but the higher-order correction to the cross section, the so-called k-factor, is determined from data.

The background from events in which a jet is misidentified as a prompt lepton, i.e. multijet background, has been modeled using data. Although the efficiency for these events is small, their contribution can not be neglected due to the large cross section. In the electron channel, we use a sample enhanced in multijet events obtained by applying less restrictive electron quality requirements. As this sample contains a fraction of events with real electrons, we do correct the multijet sample for that fraction. In the muon channel, we reverse the isolation criteria on the muon while leaving all other selection criteria unchanged to estimate a shape of the multijet background. This background is corrected for contributions already accounted for by MC by subtracting all SM contribution entering the selected multijet phase space. The normalizations in both the electron and muon channels, are determined from a fit to the $M_T^{\ell\nu}$ distribution.

3.1. *Jet Energy Calibration*

The standard jet energy scale (JES) applied to both data and MC jets, is independently determined in data and PYTHIA MC simulation, from the γ-jet balance in γ+jet events. The standard JES corrects the jet energies back to the particle level, to the energy carried by particles contained within a cone of $\Delta\mathcal{R} = 0.5$, for detector energy response, out-of-cone showering, additional $p\bar{p}$ interactions, etc. In most of the DØ analyses involving jets, an additional calibration is performed to eliminate residual calibration differences between JES-corrected jets in data and simulation. For this additional calibration, we use $Z(\to ee)$+jet events with a single jet back-to-back to the Z boson in $\Delta\phi$. Jets in the simulation are then corrected in such a way that the Z-jet p_T imbalance is matched to that observed in the data. In addition to an energy calibration, an energy smearing is performed to account for different energy resolutions in data and in MC. Possible sources of imbalance between the Z boson and the recoiling jet are soft out-of-cone radiation and inappropriate JES due to different jet flavors from those found in the derivation of the standard JES. As this additional energy calibration has been derived on ALPGEN+PYTHIA $Z(\to ee)$+jet samples, the MC correction could be considered appropriate for W+jet events generated with ALPGEN+PYTHIA as well.

This method also takes into account the jet-flavor dependence of the energy corrections i.e., the different quark-gluon composition in γ+jet and Z+jet samples. As a result, different energy corrections are obtained for quark-dominated samples such as WW, WZ, ZZ and $t\bar{t}$, and for gluon-dominated W/Z+jets MC samples.

3.2. *The Monte Carlo Corrections*

To account for differences between data and MC that arise from changes in detector efficiency and/or reconstruction algorithms over the running period, we apply correction factors to all MC samples to propagate the reconstruction and identification efficiencies of leptons and jets in data to the MC simulations. These corrections are usually at the percent level. As we also require the electron events to satisfy a single electron trigger or a trigger requiring electrons and jets, and in the muon channel we require event to be selected by one of many triggers based on leptons, jets, or their combination, we must take into account the trigger efficiency of this selection. The trigger efficiencies are measured in data and applied to simulated samples. We also adjust the instantaneous luminosity profile and the longitudinal profile of the $p\bar{p}$ interaction vertex of each MC sample to match those in data. The first improves a modeling of minimum bias effects and the latter improves the description of the distributions of kinematic quantities like the pseudorapidities of jets and the missing transverse energy. The p_T distribution of Z bosons is corrected at the generator level to reproduce dedicated measurements (see Ref. 18).

We would also like to mention some additional MC corrections based on reweighting of the MC kinematic distributions to those observed in data. Although none of these reweightings has been applied in this analysis we find it important to discuss out their implication. As it has been shown from a comparison of different generators to data (see Ref. 19), the ALPGEN generator does not reproduce the angular distributions of jets in W/Z+jets samples to be as observed in data. In particular, the observed discrepancy between the data and ALPGEN distributions is present mostly for low energetic jets, predominantly produced at higher pseudorapidities. The DØ experimental results (see Ref. 20) support these conclusions as well. The analyses with less restrictive jet selection criteria use the approach of reweighting the W/Z+jets angular jet distributions to data as it is the dominant contribution to dijet final states and its proper modeling is highly required. In the case discussed here of the W+jets analysis, the more restrictive kinematic selection removes much of the phase space in which the ALPGEN generator has difficulties in modeling data, reducing the need for the kinematic corrections of the simulation.

We do however include uncertainties due to mismodeling of some particular ALPGEN kinematic variables such as $\Delta R(jj)$, η_j of the two highest p_T jets and the W boson transverse momentum p_T^W, and perform a test in which distributions are reweighted to data to estimate the impact on final results. Due to the concern that any of these data-driven reweightings could potentially mask the presence of an excess we perform additional studies to show that this is not the case. We create a test-data set by injecting a hypothetical signal [a] of a size as reported by the CDF Collaboration into selected data and re-derive the reweightings. The ratio of the two MC reweightings, derived with and without an injected signal, is consistent with unity. Although these reweightings significantly improve the agreement between data and MC, they do not cause any of the SM processes to fill in a possible excess resonance in the dijet mass distribution.

4. Systematic Uncertainties

Systematic uncertainties taken into account in this analysis come from a large number of sources summarized in Table 1. Depending on the source, the systematic uncertainties have an impact either on the normalization or the shape of differential MC distributions tested for the presence of an excess (M_{jj} in this case). The rightmost column in Table 1 indicates whether the uncertainty only affects the normalization (N) or if it has a shape dependence (D). The impact of these uncertainties on the normalization are related to the accuracy of the theoretical cross section, luminosity measurement, triggering and reconstruction efficiencies of differ-

[a] Modeling of this signal will be described in detail further in the text.

Table 1. The amplitudes of systematic uncertainties on the MC predictions in the dijet mass distribution. The rightmost column indicates whether the uncertainty only affects the normalization (N) or if it has a shape dependence (D). (Taken from Ref. 21.)

Source of systematic uncertainty	WW+WZ+ZZ [%]	W+jets [%]	Z+jets [%]	Top [%]	Multijet [%]	Nature
Trigger/Lepton ID efficiency	±5	±5	±5	±5		N
Muon trigger correction	±5	±5	±5	±5		D
Jet identification	±1	±1	±2	±1		D
Jet energy scale	±10	±5	±7	±5		D
Jet energy resolution	±6	±1	±3	±6		D
Jet vertex confirmation	±3	±3	±4	±1		D
Luminosity	±6.1	±6.1	±6.1	±6.1		N
Cross section		±6.3	±6.3	±10		N
V+hf cross section		±20	±20			N
Multijet normalization					±20	N
Multijet shape, electron channel					±1	D
Multijet shape, muon channel					±10	D
Diboson modeling	±8					D
Parton distribution function	±1	±5	±4	±3		D
Unclustered Energy correction	± <1	±3	±3	± <1		D
ALPGEN η and $\Delta R(jet1, jet2)$ corrections		± < 1	± < 1			D
ALPGEN W p_T correction		± < 1				D
ALPGEN correction Diboson bias	±1	±1	±1	±1		D
Renormalization and factorization scales		±1	±1			D
ALPGEN parton-jet matching parameters		±1	±1			D
Parton shower and Underlying Event		±2	±2			D

ent physical processes. The impact on the M_{jj} distribution is determined by varying each parameter by its associated uncertainty (± 1 s.d.) and re-evaluating the shape of the dijet mass distribution. The values in Table 1 represent the amplitude of each systematic uncertainty on the SM predictions in the M_{jj} distribution.

As mentioned earlier, comparisons between data and MC show differences in jet η_j and $\Delta R(jj)$ distributions. Even though these differences are not so significant for the more restrictive phase space selected in this analysis, some residual differences between data and MC might still be present. A likely source for these residual differences is the ALPGEN modeling of the dominant W+jets background. Therefore, we investigate the impact of some of ALPGEN tuning parameters on the modeling of the W+jets MC such as renormalization and factorization scales, parton-matching cluster p_T threshold, and evaluate their impact on the M_{jj} distribution.

5. Study of the Dijet Mass Distribution

The predictions for the contributions from SM processes and systematic uncertainties are used in a fit of all SM contributions to data in the M_{jj} distribution. This fit minimizes a Poisson χ^2 function given in Ref. 22, with respect to variations in the rates of individual SM processes and systematic uncertainties that may modify the predicted dijet invariant mass distribution. The cross sections for dibosons and W+jets are free parameters in this fit. Systematics are treated as Gaussiandistributed uncertainties on the expected numbers of events. The fit computes the optimal central values for the systematic uncertainties, while accounting for departures from the nominal predictions by including a term in the χ^2 function that sums the squared deviation of each systematic in units normalized by its ± 1 s.d. uncertainties. The M_{jj} distribution after the fit is consistent with the SM prediction and does not show a preference for an excess of events of the size observed in the CDF data as shown in Fig. 1. The number of predicted events of 12790 ± 214 is in agreement with the observed one of 12879 events. The impact of data-driven

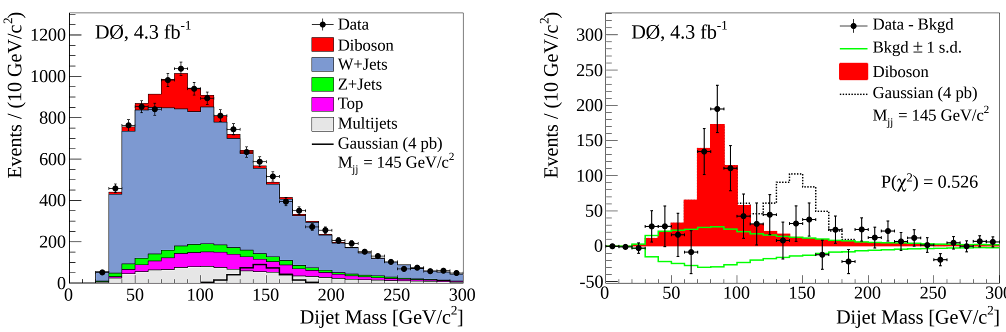

Fig. 1. (Left) Comparison of SM contributions to data after the fit, and (right) comparison of data after subtraction of SM contributions other than that from dibosons, with the ± 1 s.d. on all SM predictions. Contributions are shown for the electron and muon channels combined. These distributions do not have the additional kinematic corrections applied to the ALPGEN MC. (Taken from Ref. 23.)

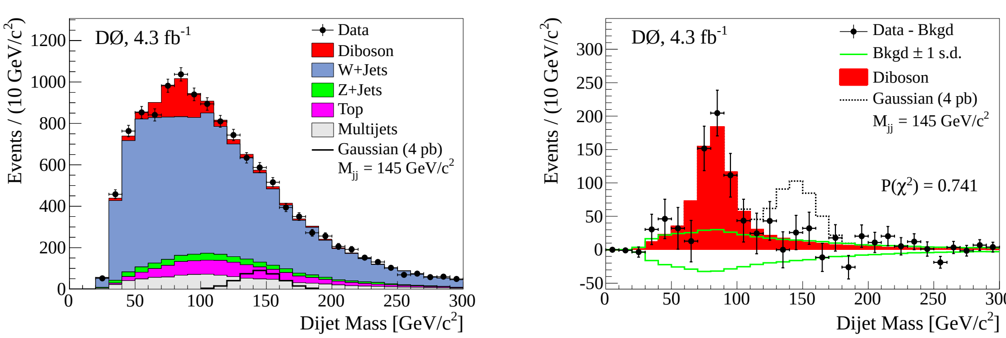

Fig. 2. (Left) Comparison of SM contributions to data after the fit, and (right) comparison of data after subtraction of SM contributions other than that from dibosons, with the ± 1 s.d. on all SM predictions. Contributions are shown for the electron and muon channels combined. These distributions have the additional kinematic corrections applied to the ALPGEN MC. (Taken from Ref. 23.)

modeling corrections on W+jets that we discussed earlier in the text is shown Fig. 2

where one can see that the χ^2 fit probability (P(χ^2)) improves when the $\Delta R(jj)$, η_j and p_T^W distributions are corrected.

6. Modeling of a Hypothetical Dijet Mass Resonance

As no obvious excess is found in the dijet mass distribution, we proceed with setting limits on the production cross section for the hypothetical $WX \to \ell\nu jj$ process. We model the dijet mass resonance at 145 GeV/c^2 using a simple Gaussian model. The width of this dijet resonance is estimated from the expected resolution of the DØ detector as $\sigma_{X\to jj} = \sigma_{W\to jj} \cdot \sqrt{M_{X\to jj}/M_{W\to jj}} = 15.7$ GeV/c^2, where $\sigma_{W\to jj}$ and $M_{W\to jj}$ are the width and mass of the $W \to jj$ resonance, determined to be $\sigma_{W\to jj} = 11.7$ GeV/c^2 and $M_{W\to jj} = 81$ GeV/c^2 from a simulation of $WW \to \ell\nu jj$ production, and $M_{jj} = 145$ GeV/c^2 is a mean value of the hypothetical dijet mass resonance. When performing tests at other M_{jj} values, the width is adjusted accordingly. The efficiency of the hypothetical process $WX \to \ell\nu jj$, is estimated from a MC simulation of $WH \to \ell\nu b\bar{b}$ production. When testing the Gaussian signal with a mean of $M_{jj} = 145$ GeV/c^2, the efficiency is taken from the $WH \to \ell\nu b\bar{b}$ simulation with $M_H = 150$ GeV/c^2. This prescription is chosen to be consistent with the CDF analysis. For other values of M_{jj} that we test in a range of 110 GeV/c^2-170 GeV/c^2, we use the efficiencies obtained for $WH \to \ell\nu b\bar{b}$ MC events with a value of M_H offset by 5 GeV/c^2. The efficiency for WH samples with $M_H > 150$ GeV/c^2 is estimated by extrapolating a polynomial fit to the values in the range 90 GeV/c^2 - 150 GeV/c^2.

The systematic uncertainties assigned to the modeling of the $WX \to \ell\nu jj$ signal are derived following the behavior of the WW MC sample. The signal is assigned uncertainties for luminosity and lepton and jet identifications. The uncertainty on the jet resolution is derived by changing the width of the Gaussian by ±3% with a corresponding change in rate of ±0.7%. The JES uncertainty is modeled by shifting the mean of the Gaussian by ±1.5% with a corresponding ±2% change in rate.

We include this $WX \to \ell\nu jj$ signal with a hypothetical $X \to jj$ dijet mass resonance in the M_{jj} fit, where the diboson, W+jets and WX cross sections are fit with no constraint. The dijet mass distributions after the fit, analogous to those in Fig. 1 are shown in Fig. 3. The yellow contribution in Fig. 3 corresponds to the WX signal as obtained from the best fit value and yields the production cross section of $\sigma(p\bar{p} \to WX) = 0.82^{+0.83}_{-0.82}$ pb. The fitted cross section is consistent with zero excess. If we repeat the fit in the same manner as CDF, where we fix the diboson cross section to the SM prediction with a Gaussian prior of 7% on the cross section, we measure the cross section of $\sigma(p\bar{p} \to WX) = 0.42^{+0.76}_{-0.42}$ pb which is also consistent with no excess.

7. Setting Limits

To estimate the size of the signal that could potentially be present in the DØ data we proceed with setting 95% confidence level (C.L.) upper limits on the production

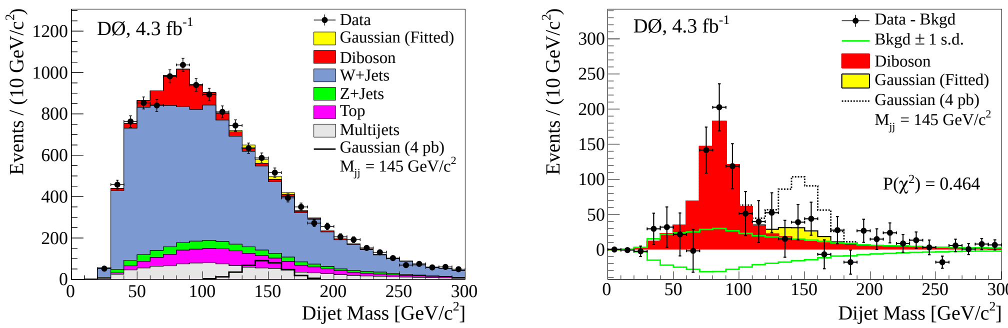

Fig. 3. (Left) Comparison of SM contributions to data after the fit, and (right) comparison of data after subtraction of SM contributions other than that from dibosons, and WX (yellow), with the ±1 s.d. on all SM predictions. Contributions are shown for the electron and muon channels combined. These distributions do not have the additional kinematic corrections applied to the ALPGEN MC. (Taken from Ref. 21.)

cross section of a hypothetical $WX \to \ell\nu jj$ process. We set 95% C.L. limits for Gaussian signals with mean dijet invariant masses in the range 110 GeV/$c^2 < M_{jj} <$ 170 GeV/c^2, in steps of 5 GeV/c^2. Limits are calculated using the CL_s method with a negative log-likelihood ratio (LLR) test statistic as defined in Ref. 24 - 26. The value of CL_s is defined as $CL_s = CL_{s+b}/CL_b$ where CL_{s+b} and CL_b are the confidence levels for the signal-plus-background and the background-only hypotheses, respectively. We fit the signal-plus-background and the background-only hypotheses to data and to pseudo-experiments generated from Poisson fluctuations, allowing for statistical and systematic fluctuations of the SM contributions and allowing the cross sections for W+jets production to float with no constraint. Other contributions are constrained by their assigned uncertainties as given in Table 1. The results of the fit from each pseudo-experiment are used to generate the expected LLR distribution for each mass hypothesis. The LLR provides a sensitive measure of model compatibility, providing information on both the rate and mass of any signal-like excess. We then study the LLR distributions obtained with actual data. The results of the LLR test in Fig. 4 show a difference between the two hypotheses, demonstrating that in data, no significant excess is observed. The confidence levels are then derived from the semi-infinite bound integration of the corresponding LLR distributions for the signal-plus-background and the background-only hypotheses.

The results are shown in Fig. 4 and summarized in Table 2. For a resonance at

Table 2. Expected and observed 95% C.L. upper limits on the cross section for a dijet invariant mass resonance. (Taken from Ref. 23.)

M_{jj} [GeV/c^2]	110	115	120	125	130	135	140	145	150	155	160	165	170
Expected [pb]	2.20	2.01	1.90	1.78	1.71	1.64	1.58	1.52	1.47	1.40	1.37	1.31	1.24
Observed [pb]	2.57	2.44	2.35	2.27	2.19	2.09	2.00	1.85	1.69	1.58	1.46	1.36	1.28

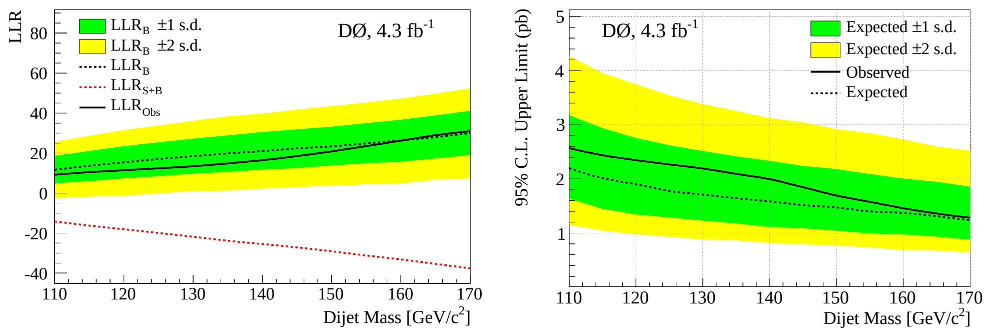

Fig. 4. (Left) LLR test statistic as a function of M_{jj}. Shown are the expected LLR for the background-only hypothesis with regions corresponding to a 1 s.d. and 2 s.d. fluctuation of the backgrounds, for the signal+background prediction, and for the data. (Right) The 95% C.L. upper limits on the cross section for a Gaussian signal in dijet invariant mass. Shown are the limits expected using the background prediction, and the observed data. The regions corresponding to a 1 s.d. and 2 s.d. fluctuation of the backgrounds are also shown. The figure to the right is taken from Ref. 23.

$M_{jj} = 145$ GeV/c^2 modeled as in the CDF analysis we set a 95% CL upper limit of 1.9 pb on the production cross section.

In addition, we report the significance evaluated from the p-value obtained via integration of signal+background LLR distributions above the observed LLR i.e., the probability for the signal+background hypothesis to be true. This p-value as a function of a WX cross section is shown in Fig. 5. The calculated p-value for a Gaussian signal with cross section of 4 pb is 8.0×10^{-6}, which corresponds to a rejection at 4.3 s.d.

7.1. *Signal-Injected Data*

In a further effort to explore the possibility that there is a signal of the type claimed by CDF, we study what the statistical tests would show if the DØ data had a signal of the type claimed by CDF. To test this possibility, we create a signal-injected mock sample, i.e. a data sample plus the hypothetical Gaussian signal model normalized to a cross section of 4 pb. The size and shape of the injected Gaussian model for $M_{jj} = 145$ GeV/c^2 relative to other SM contributions is shown in Fig. 1 and Fig. 2. First, we perform the χ^2 fit, fitting only the diboson and W+jets cross sections with no constraint, and without the WX contribution included in the fit. The resulting P(χ^2) value reflects poor agreement between signal-injected data and SM predictions. Then we perform the χ^2 fit with the WX included and fit the diboson, W+jets and WX cross sections with no constraint. By construction the fit results in the WX cross section consistent with 4 pb, and its distribution is presented in Fig. 6. The P(χ^2) values in Fig. 6 clearly indicate improved agreement between signal-injected data and all simulations when the WX signal is included in the fit.

Further, we calculate LLR values for this scenario as a function of M_{jj},

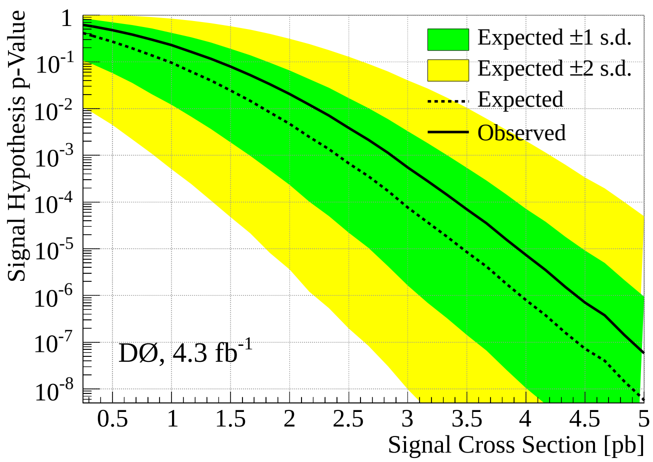

Fig. 5. p-value for pseudo-experiments drawn from the signal+background hypothesis with signal given as a Gaussian dijet mass resonance at $M_{jj} = 145$ GeV$/c^2$ using the CDF proposed modeling. (Taken from Ref. 23.)

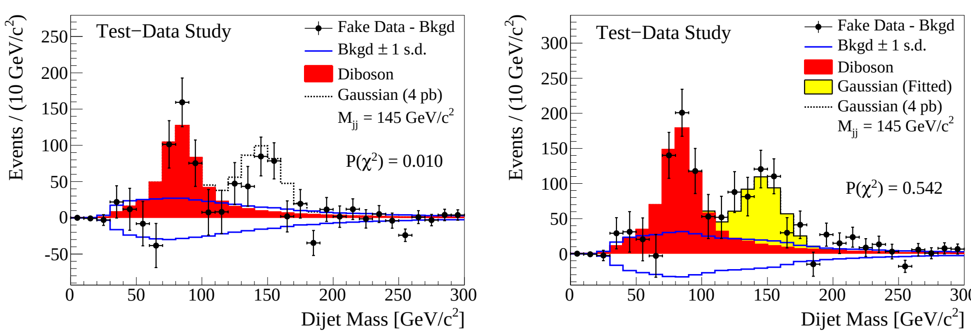

Fig. 6. Comparison of signal-injected data after subtraction of SM contributions (other than that from dibosons) (left) to the diboson SM prediction, and (right) to the diboson SM prediction and WX (yellow), with the ± 1 s.d. on all SM predictions. Contributions are shown for the electron and muon channels combined. These distributions do not have the additional kinematic corrections applied to the ALPGEN MC.

testing with a Gaussian signal at every 5 GeV in the range 110 GeV$/c^2 < M_{jj} < 170$ GeV$/c^2$. The LLR comparison for different hypotheses is shown in Fig. 7, demonstrating that this analysis is sensitive to the artificially injected excess. Because the signal+background hypotheses are significantly different for the signal-injected and observed data, this test confirms our ability to detect the signal reported by the CDF Collaboration, had it been present in DØ data.

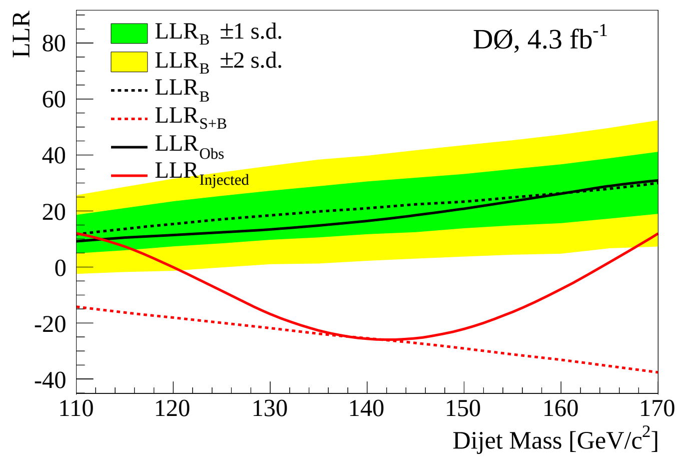

Fig. 7. LLR test statistic as a function of M_{jj}. Shown are the expected LLR for the background-only hypothesis with regions corresponding to a 1 s.d. and 2 s.d. fluctuation of the backgrounds, for the signal+background prediction, for the data, and for data with a dijet mass resonance at 145 GeV/c^2 injected with a cross section of 4 pb. (Taken from Ref. 23.)

8. Summary

We have used 4.3 fb^{-1} of integrated luminosity collected at the DØ experiment to study the M_{jj} spectrum in $\ell\nu jj$ events. Following the analysis strategy of the CDF Collaboration as closely as possible, we find no evidence for an anomalous resonant production of dijets in the mass range 110 GeV/c^2 - 170 GeV/c^2. We set a 95% C.L. upper limit of 1.9 pb on the cross section for a hypothetical WX signal with a mass resonance at 145 GeV/c^2 and present the variation of our p-value for exclusion of potential resonance cross sections other than 4 pb.

Acknowledgments

We thank the staffs at Fermilab and collaborating institutions, and acknowledge support from the DOE and NSF (USA); CEA and CNRS/IN2P3 (France); FASI, Rosatom and RFBR (Russia); CNPq, FAPERJ, FAPESP and FUNDUNESP (Brazil); DAE and DST (India); Colciencias (Colombia); CONACyT (Mexico); KRF and KOSEF (Korea); CONICET and UBACyT (Argentina); FOM (The Netherlands); STFC and the Royal Society (United Kingdom); MSMT and GACR (Czech Republic); CRC Program and NSERC (Canada); BMBF and DFG (Germany); SFI (Ireland); The Swedish Research Council (Sweden); and CAS and CNSF (China).

References

1. P. H. Frampton and S. L. Glashow, *Phys. Lett. B* **190**, 157 (1987).
2. U. Baur, I. Hinchliffe and D. Zeppenfeld, *Int. J. Mod. Phys. A* **2**, 1285 (1987).
3. U. Baur, M. Spira and P. M. Zerwas, *Phys. Rev. D* **42**, 815 (1990).

4. T. Aaltonen *et al.* (CDF Collaboration), *Phys. Rev. Lett.* **106**, 171801 (2011).
5. T. Aaltonen *et al.* (CDF Collaboration), *Phys. Rev. Lett.* **104**, 101801 (2010).
6. T. Aaltonen *et al.* (CDF Collaboration), http://www-cdf.fnal.gov/physics/ewk/2011/wjj/7_3.html.
7. G. C. Blazey *et al.*, arXiv:hep-ex/0005012 (2000).
8. T. Sjöstrand, S. Mrenna and P. Skands, *J. High Energy Phys.* **0605**, 026 (2006). Version 6.409 is used.
9. J. Pumplin *et al.*, *J. High Energy Phys.* **07**, 12 (2002).
10. J. Pumplin *et al.*, *J. High Energy Phys.* **10**, 46 (2003).
11. J. M. Campbell and R. K. Ellis, *Phys. Rev. D* **60**, 113006 (1999). Version 6.0 is used.
12. M. L. Mangano *et al.*,*J. High Energy Phys.* **07**, 001 (2003). Version 2.11 is used with the $W+c$ fix from v2.12.
13. E. Boos *et al.*, *Nucl. Instrum. Methods Phys. Res. A* **534**, 250 (2004).
14. R. Gavin, Y. Li, F. Petriello and S. Quackenbush, *Comput. Phys. Commun.* **182**, 2388 (2011).
15. J. M. Campbell and R. K. Ellis, *Phys. Rev. D* **65**, 113007 (2002).
16. S. Moch and P. Uwer, *Phys. Rev. D* **78**, 034003 (2008).
17. N. Kidonakis, *Phys. Rev. D* **74**, 114012 (2006).
18. V. M. Abazov *et al.*, *Phys. Rev. Lett.* **100**, 102002 (2008).
19. J. Alwall *et al.*, *Eur. Phys. C* **53**, 473 (2008).
20. V. M. Abazov *et al.* (D0 Collaboration), *Phys. Lett. B* **682**, 370 (2010).
21. http://prl.aps.org/supplemental/PRL/v107/i1/e011804.
22. W. Fisher, FERMILAB-TM-2386-E, 2006 (unpublished).
23. V. M. Abazov *et al.* (D0 Collaboration), *Phys. Rev. Lett.* **107**, 011804 (2011).
24. T. Junk, *Nucl. Intrum. Meth. A* **434**, 435 (1999).
25. A. Read, CERN-2000-005, 2000 (unpublished).
26. W. Fisher, DØ Note 4975, 2005 (unpublished).